

## Asymmetric Hydroformylation of Olefins with Rh Catalysts Modified with Chiral Phosphine–Phosphite Ligands

Miguel Rubio,<sup>†</sup> Andrés Suárez,<sup>†</sup> Eleuterio Álvarez,<sup>†</sup> Claudio Bianchini,<sup>‡</sup>  
Werner Oberhauser,<sup>‡</sup> Maurizio Peruzzini,<sup>\*,‡</sup> and Antonio Pizzano<sup>\*,†</sup>

*Instituto de Investigaciones Químicas, Consejo Superior de Investigaciones Científicas and Universidad de Sevilla, Avda Américo Vespucio n° 49, Isla de la Cartuja, 41092 Sevilla, Spain, and Istituto di Chimica dei Composti Organometallici (ICCOM-CNR), Area di Ricerca CNR di Firenze, via Madonna del Piano 10, 50019 Sesto Fiorentino (FI), Italy*

Received July 23, 2007

Rhodium complexes stabilized by modularly designed chiral phosphine–phosphite ligands (P–OP) have been tested in the asymmetric hydroformylation of styrene, vinyl naphthalenes, and allyl cyanide. Based on single-crystal X-ray diffraction analysis and NMR studies, restricted aryl rotation has been found to characterize ligands **1e** and **1f**. The outcome of the rhodium-catalyzed hydroformylation reactions is highly dependent on the nature of the two coordinating functions of the phosphine–phosphite and of the ligand backbone as well. Among the ligands studied, those with an oxyphenylene backbone and PAr<sub>2</sub> ends gave the best results, outperforming those with *P*-stereogenic phosphine groups. The 1-naphthyl-substituted catalyst brought about the hydroformylation of styrene with a 71% ee, while the xylyl catalyst afforded the best results in the hydroformylation of allyl cyanide, yielding an iso/*n* ratio of 13 and 53% ee in the branched isomer. Several hydrido(carbonyl) species of the formula RhH(CO)<sub>2</sub>(P–OP) have been generated by reacting Rh(acac)(CO)<sub>2</sub>/P–OP with syngas. In situ high-pressure NMR experiments showed the phosphine group to occupy an apical position of the trigonal bipyramidal coordination geometry, which allows an aryl–aryl interaction between the phosphine substituents and the substrate during the hydroformylation of vinyl arenes. In line with this finding, a remarkable enantioselectivity of 89% ee was obtained with the naphthyl catalyst and 1-vinyl naphthalene as substrate.

### Introduction

The enantioselective hydroformylation of prochiral alkenes is one of the most challenging processes in asymmetric catalysis. Indeed, a strict control of enantio-, chemo-, and regioselectivity is required to efficiently produce the desired branched isomer in high optical purity.<sup>1</sup> Motivated by the convenience of this process to obtain synthetically valuable aldehydes, extensive studies with several types of catalysts have been developed.<sup>2</sup> Among the many catalysts investigated, those based on Rh and chelating phosphorus ligands have shown superior activity and selectivity.<sup>3–5</sup> A vast range of P-ligands have been tested, but only very few of them have provided high enantioselectivity in

the carbonylation of olefins. From a perusal of the best-performing P-ligands, one may conclude that these ligands do not share many common characteristics: they are often structurally diverse with different symmetries (*C*<sub>1</sub> or *C*<sub>2</sub>) and contain various types of phosphorus donor groups like phosphines, phosphoramidites, or phosphites. For instance, azaphospholanes<sup>6</sup> and diphosphites<sup>7</sup> have been shown to generate very efficient rhodium catalysts for the hydroformylation of vinyl arenes, vinyl acetate, and allyl cyanide. Likewise, a recently reported phenyl-substituted bisphospholane has also provided excellent results.<sup>8</sup> Moreover, Zhang has recently described a binaphthyl-based phosphine–phosphoramidite ligand capable of inducing an excellent enantioselectivity in the hydroformylation of several olefins.<sup>9</sup> In terms of catalyst scope, the work developed by Takaya and Nozaki with the BINAPHOS ligands occupies a prominent place in this field. By using these phosphine–phosphites, a wide variety of olefins, encompassing vinyl arenes, enamides, enol esters, heterocyclic olefins, dienes, or vinyl

\* Corresponding authors. E-mail: mperuzzini@iccom.cnr.it (M.P.); pizzano@iiq.csic.es (A.P.).

<sup>†</sup> Universidad de Sevilla.

<sup>‡</sup> ICCOM-CNR.

(1) (a) *Homogeneous Catalysis: Understanding the Art*; van Leeuwen, P. W. N. M., Ed.; Kluwer Academic Publishers: Dordrecht, 2004. (b) Nozaki, K. In *Comprehensive Asymmetric Catalysis*; Jacobsen, E. N., Pfaltz, A., Yamamoto, H., Eds.; Springer: Berlin, 1999; Vol. 1. (c) Consiglio, C. In *Catalytic Asymmetric Catalysis*; Ojima, I., Ed.; VCH: New York, 1993.

(2) (a) Agbossou, F.; Carpentier, J.-F.; Mortreux, A. *Chem. Rev.* **1995**, *95*, 2485. (b) Gladiali, S.; Bayón, J. C.; Claver, C. *Tetrahedron: Asymmetry* **1995**, *6*, 1453.

(3) Other catalysts with either Rh complexes based on different ligands or Pt/Sn systems have been studied in detail.<sup>4,5</sup>

(4) (a) Stille, J. K.; Su, H.; Brechot, P.; Parrinello, G.; Hegedus, L. S. *Organometallics* **1991**, *10*, 1183. (b) Casey, C. P.; Martins, S. C.; Fagan, M. A. *J. Am. Chem. Soc.* **2004**, *126*, 5585.

(5) (a) Arena, D. G.; Nicoló, F.; Drommi, D.; Bruno, G.; Faraone, F. *J. Chem. Soc., Chem. Commun.* **1994**, 2251. (b) Castellanos-Páez, A.; Castellón, S.; Claver, C. *J. Organomet. Chem.* **1997**, *539*, 1.

(6) (a) Clark, T. P.; Landis, C. R.; Freed, S. L.; Klosin, J.; Abboud, K. A. *J. Am. Chem. Soc.* **2005**, *127*, 5040. (b) Breeden, S.; Cole-Hamilton, D. J.; Foster, D. F.; Schwarz, G. J.; Wills, M. *Angew. Chem., Int. Ed.* **2000**, *39*, 4106.

(7) (a) Babin J. E.; Whiteker, G. T. WO 93/0389, U.S. Patent US911-518, 1992. (b) Diéguez, M.; Pàmies, O.; Ruiz, A.; Castellón, S.; Claver C. *Chem. Eur. J.* **2001**, *7*, 3086. (c) Buisman, G. J. H.; van der Veen, L. A.; Klootwijk, A.; de Lange, W. G. J.; Kamer, P. C. J.; van Leeuwen, P. W. N. M.; Vogt, D. *Organometallics* **1997**, *16*, 2929. (d) Copley, C. J.; Froese, R. D. J.; Klosin, J.; Qin, C.; Whiteker, G. T.; Abboud, K. A. *Organometallics* **2007**, *26*, 2986.

(8) Axtell, A. T.; Copley, C. J.; Klosin, J.; Whiteker, G. T.; Zanotti-Gerosa, A.; Abboud, K. A. *Angew. Chem., Int. Ed.* **2005**, *44*, 5834.

(9) Yan, Y.; Zhang, X. *J. Am. Chem. Soc.* **2006**, *108*, 7198.

$\beta$ -lactams, were hydroformylated with generally high levels of regio- and enantioselectivity.<sup>10</sup> These outstanding results have attracted much interest on phosphine–phosphites for the enantioselective hydroformylation of olefins, and several new ligand families of this type have been prepared and tested.<sup>11</sup> Although some of these ligands share  $\text{PAR}_2$  and  $\text{P(OAr)}_2$  groups with BINAPHOS, lower enantioselectivities are generally obtained, which reflects the great influence of the ligand backbone in driving the reaction outcome.

In our laboratories, we are studying the application of phosphine–phosphites in asymmetric hydrogenation reactions. To this purpose, a modular synthesis of phosphine–phosphite ligands, containing phenylene or ethylene bridges, has been developed.<sup>12</sup> The easily tunable structure of these compounds has been fruitfully exploited in the reduction of several olefins and imines.<sup>13</sup>

Herein, we report on the use of rhodium catalysts modified with chiral phosphine–phosphite ligands in the hydroformylation of vinyl arenes and allyl cyanide that are capable of inducing enantioselectivities as high as 89% ee. In situ high-pressure NMR studies (HP-NMR) have provided valuable information on the course of the catalytic process.

## Results and Discussion

**Ligand Features.** The phosphine–phosphite ligands used in this study are shown in Figure 1. Ligands of type **1** contain a phenylene backbone connecting the phosphine and phosphite donor atoms. They possess a bulky phosphite group and differ from each other in the substituents on the phosphine P-atom. All ligands have been previously described, except for the novel naphthyl derivative **1f** (Scheme 1) synthesized from *o*-anisyl-di(1-naphthyl)phosphine.<sup>14</sup> The phosphine–phosphite ligands of type **2** bear a less bulky phosphite group, while a more flexible ethylene bridge features ligand **3**. Finally, ligands **4** and **5** contain *P*-stereogenic phosphine groups.

Broad signals were observed in the  $^{31}\text{P}\{^1\text{H}\}$  spectrum of ligand **1f** at room temperature. Heating the sample to 40 °C narrowed the phosphine signal and allowed the observation of the  $^2J_{\text{PP}}$  (40 Hz) coupling constant, while the phosphite signal remained broad. Moreover, the *o*-tolyl ligand **1e** displayed two broad signals at room temperature that sharpened into doublets ( $^2J_{\text{PP}} = 36$  Hz) upon warming at 40 °C. Interestingly, compounds **1a** and **1d**, whose aryl rings can rotate easily around the P–C bonds, showed sharp doublets. In view of these findings, we interpret the solution behavior of ligands **1e** and

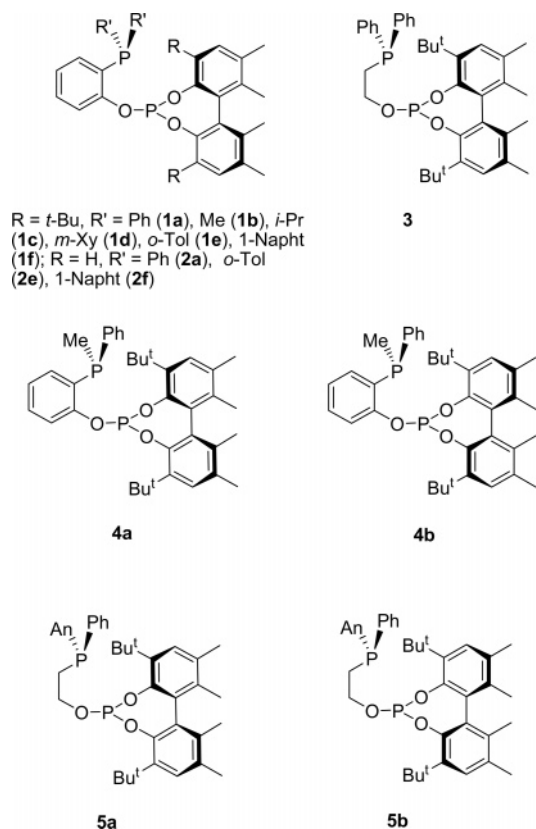
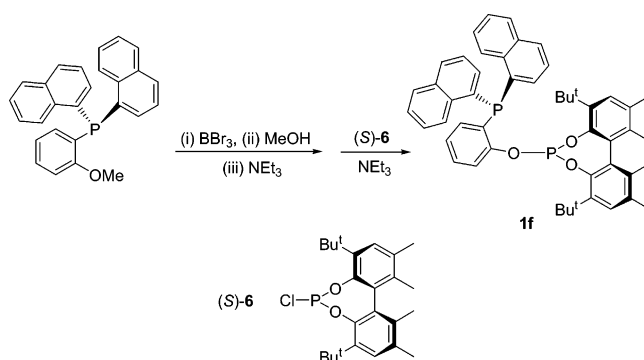


Figure 1.

## Scheme 1



**1f** as due to a slow interconversion between rotational isomers. This feature seems to be generated by steric effects, as ligands **2e** and **2f**, which possess a smaller phosphite group, showed only sharp signals.<sup>13d</sup> Aware of the impact that the structure of the  $\text{PAR}_2$  group may have on the catalytic performance of these ligands,<sup>12b</sup> we first tried to gain additional information about the observed restricted rotation. To this purpose, the solid-state structures of **1a** and **1e** in the complexes  $\text{PdCl}_2(\text{P-OP})[\text{P-OP} = \mathbf{1a} (\mathbf{7a}), \mathbf{1e} (\mathbf{7e})]$  have been determined by single-crystal X-ray diffraction analyses and compared to each other. Complexes **7** were straightforwardly prepared by adding a stoichiometric amount of the appropriate phosphine–phosphite ligand to a toluene solution of  $\text{PdCl}_2(\text{MeCN})_2$  (see Experimental Section for details).

Figures 2 and 3 show ORTEP representations of these complexes along with selected bond distances and angles. The structure of compound **7a** is very similar to that previously determined for  $\text{RhCl}(\text{CO})(\mathbf{1a})$ , especially in regards to the

(10) (a) Sakai, N.; Mano, S.; Nozaki, K.; Takaya, H. *J. Am. Chem. Soc.* **1993**, *115*, 7033. (b) Nozaki, K.; Sakai, N.; Nanno, T.; Higashijima, T.; Mano, S.; Horiuchi, T.; Takaya, H. *J. Am. Chem. Soc.* **1997**, *119*, 4413. (c) Horiuchi, T.; Ohta, T.; Shirakawa, E.; Nozaki, K.; Takaya, H. *J. Org. Chem.* **1997**, *62*, 4285. (d) Nozaki, K.; Li, W.; Horiuchi, T.; Takaya, H. *J. Org. Chem.* **1996**, *61*, 7658. (e) Horiuchi, T.; Ohta, T.; Nozaki, K.; Takaya, H. *Chem. Commun.* **1996**, 155. (f) Sakai, N.; Nozaki, K.; Takaya, H. *J. Chem. Soc., Chem. Commun.* **1994**, 4285.

(11) (a) Deerenberg, S.; Kamer, P. C. J.; van Leeuwen, P. W. N. M. *Organometallics* **2000**, *19*, 2065. (b) Pàmies, O.; Net, G.; Ruiz, A.; Claver, C. *Tetrahedron: Asymmetry* **2002**, *12*, 3441. (c) Kless, A.; Holz, J.; Heller, D.; Kadyrov, R.; Selke, R.; Fischer, C.; Börner, A. *Tetrahedron: Asymmetry* **1996**, *7*, 33.

(12) (a) Suárez, A.; Méndez-Rojas, M. A.; Pizzano, A. *Organometallics* **2002**, *21*, 4611. (b) Vargas, S.; Rubio, M.; Suárez, A.; del Río, D.; Álvarez, E.; Pizzano, A. *Organometallics* **2006**, *25*, 961.

(13) (a) Rubio, M.; Suárez, A.; Álvarez, E.; Pizzano, A. *Chem. Commun.* **2005**, 628. (b) Suárez, A.; Pizzano, A. *Tetrahedron: Asymmetry* **2001**, *12*, 2501. (c) Vargas, S.; Rubio, M.; Suárez, A.; Pizzano, A. *Tetrahedron Lett.* **2005**, *46*, 2049. (d) Rubio, M.; Vargas, S.; Suárez, A.; Álvarez, E.; Pizzano, A. *Chem. Eur. J.* **2007**, *13*, 1821.

(14) Laitinen, R. H.; Haukka, M.; Koskinen, A. M. P.; Koskianen, J. *J. Organomet. Chem.* **2000**, *598*, 235.

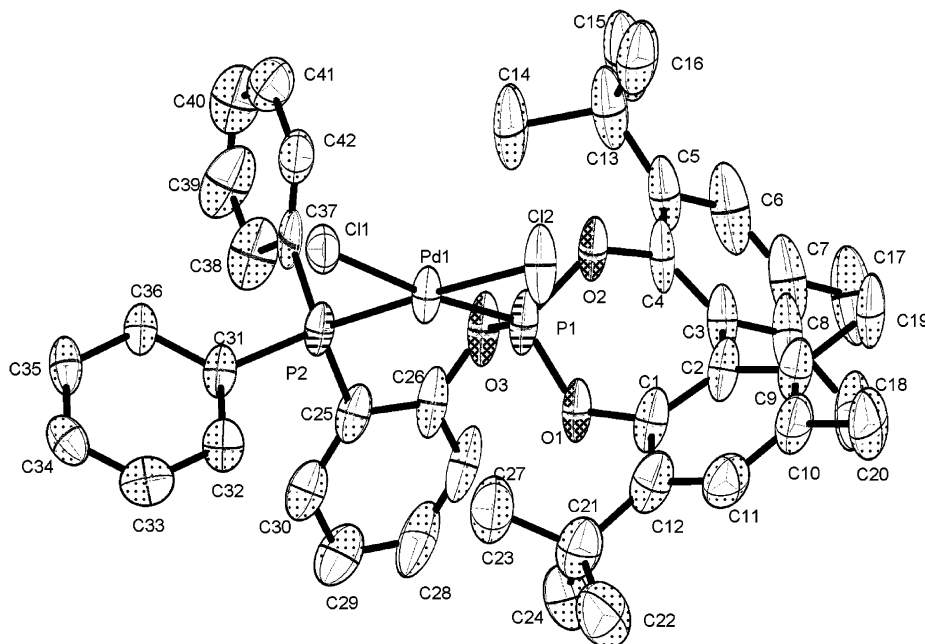


**Figure 2.** ORTEP drawing of complex **7a**. Selected bond distances [ $\text{\AA}$ ] and angles [deg]: Pd(1)–P(1) = 2.1948(18), Pd(1)–P(2) = 2.2659(17), Pd(1)–Cl(1) = 2.3172(16), Pd(1)–Cl(2) = 2.3341(18); P(1)–Pd(1)–P(2) = 90.38(6), P(1)–Pd(1)–P(2)–C(37) =  $-84.9(2)$ , P(1)–Pd(1)–P(2)–C(31) = 151.3(3).

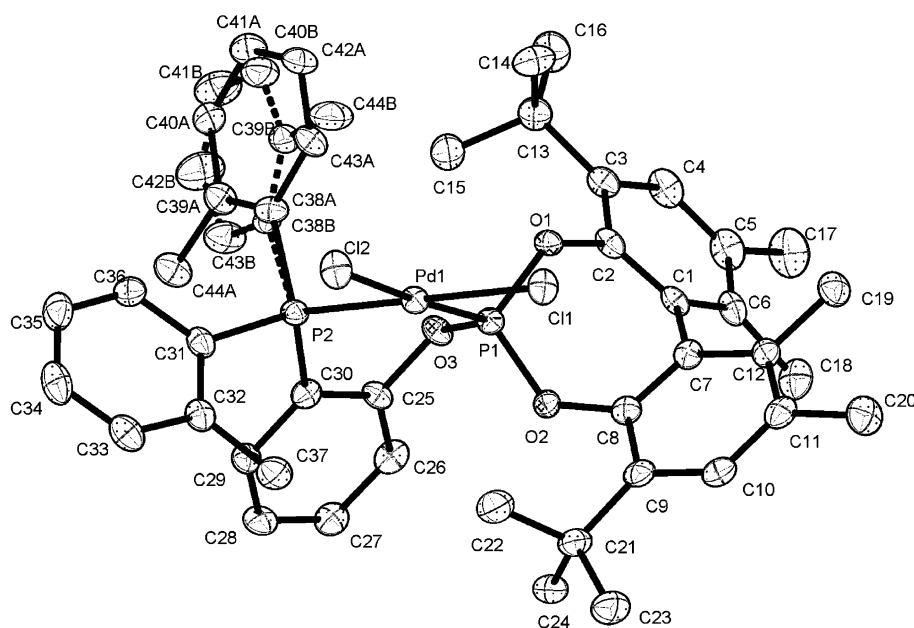


**Figure 3.** ORTEP drawing of complex **7e**. A and B denote the two rotational isomers. Selected bond distances [ $\text{\AA}$ ] and angles [deg]: Pd(1)–P(1) = 2.1933(8), Pd(1)–P(2) = 2.2717(8), Pd(1)–Cl(1) = 2.3407(8), Pd(1)–Cl(2) = 2.3469(7); P(1)–Pd(1)–P(2) = 90.44(3), P(1)–Pd(1)–P(2)–C(38A) =  $-85.45(19)$ , P(1)–Pd(1)–P(2)–C(38B) =  $-75.09(18)$ , P(1)–Pd(1)–P(2)–C(31) = 156.69(11).

conformation of **1a**, and, for this reason, it does not deserve any further comment. In contrast, complex **7e** coexists in the solid state as a 1:1 mixture of two rotational isomers, differing from each other in the orientation of the pseudoaxial *o*-tolyl group<sup>15</sup> with the methyl substituent pointing either to the Pd atom or to the backbone. Noteworthy, the rest of the structure is practically coincident in the two rotamers as well as with the structure of **7a**. Likewise, the <sup>1</sup>H and <sup>31</sup>P{<sup>1</sup>H} NMR spectra of **7e** showed the existence of two species in solution, identified

by two groups of signals in a 1.5:1 ratio. An analysis of the <sup>1</sup>H NMR spectra acquired at different temperatures showed the coalescence of homologous methyl signals of the two isomers (Figure 4) with the exception of one methyl substituent of a tolyl fragment that did not reach the fast exchange regime even at the higher temperature investigated. Interestingly, the resonances of this group in either isomer show an important difference in chemical shift (ca. 1.8 ppm), suggesting a significantly different environment for this substituent in the two species. A perusal of the X-ray structure of **7e** indicates that this methyl group may be that located in the pseudoaxial tolyl ring (C44). Moreover, as C44A points directly to the phenylene backbone, one would expect a considerable shielding

(15) For other examples of structures with *o*-tolyl phosphines, see: (a) Tsuruta, H.; Imamoto, T.; Yamaguchi, K.; Gridnev, I. D. *Tetrahedron Lett.* **2005**, *46*, 2879. (b) Casas, J. M.; Forniés, J.; Fuertes, S.; Martín, A.; Sicilia, V. *Organometallics* **2007**, *26*, 1674.

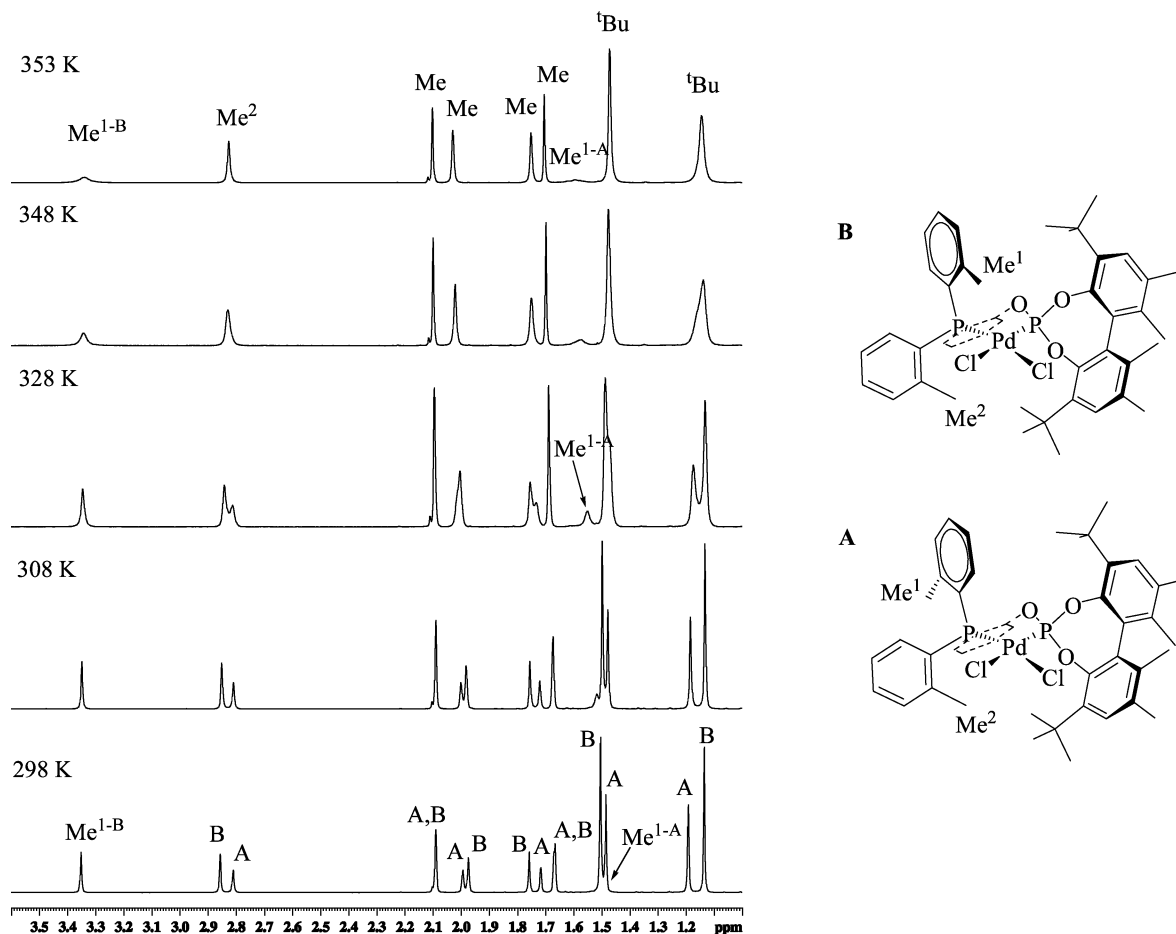


**Figure 4.** Methyl region of  $^1\text{H}$  NMR spectrum of complex **7e** ( $\text{C}_6\text{D}_6$ , 500 MHz), registered at different temperatures. **A** and **B** refer to the two isomers observed in the X-ray structure.

**Table 1. Styrene Hydroformylation with Catalysts Based on P–OP Ligands<sup>a</sup>**

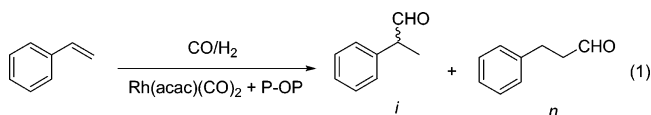
entry	P–OP	% conversion (time)	i:n	% ee (conf.)
1	<b>1a</b>	93 (24 h)	98:2	43 (S)
2	<b>1b</b>	34 (48 h)	98:2	25 (R)
3	<b>1c</b>	55 (18 h)	93:7	32 (R)
4	<b>1d</b>	97 (24 h)	98:2	47 (S)
5	<b>1e</b>	28 (24 h)	96:4	33 (S)
6	<b>1f</b>	48 (24 h)	98:2	71 (S)
7	<b>2a</b>	7 (24 h)	n.d.	n.d.
8	<b>3</b>	100 (24 h)	96:4	25 (R)
9	<b>4a</b>	85 (16 h)	97:3	39 (S)
10	<b>4b</b>	47 (18 h)	96:4	28 (R)
11	<b>5a</b>	100 (24 h)	94:6	25 (R)
12	<b>5b</b>	94 (24 h)	93:7	19 (S)

<sup>a</sup> Reactions were carried out at 50 °C with an initial gas pressure of 20 bar, in toluene at a S/C = 1000 in a 750 mL reaction vessel. Conversion was determined by  $^1\text{H}$  NMR and enantiomeric excess (ee) by chiral GC. Configuration was determined by comparison of optical rotation to the literature value.

for this group.<sup>16</sup> On this basis, it is reasonable to assign the singlet at 1.50 ppm to the rotamer **A**. Conversely, the singlet at  $\delta$  3.35 can be ascribed to compound **B**, which is the preferred isomer in solution.

**Catalytic Hydroformylation Reactions.** Styrene hydroformylation reactions (eq 1) were carried out in toluene at 50 °C with a substrate to catalyst ratio (S/C) of 1000 and at an initial pressure of 20 bar. The results obtained are summarized in Table 1. The experiments were carried out in a 750 mL Parr

vessel containing a rack for six glass tubes to run parallel catalytic reactions. No significant decrease in the gas pressure was observed during the whole reaction.



An examination of the results obtained indicates that the catalyst performance is very sensitive to the ligand employed. Indeed, the conversion obtained with ligands of type **1** ranges between 28% (**1e**, entry 5) and 97% (**1d**, entry 4) for the same reaction time. The well-known effect due to bulky phosphites on the catalyst activity<sup>17</sup> is highlighted by a comparison of the reactions catalyzed by Rh complexes modified with **1a** and **2a** (entries 1, 7). The effect is opposite on the phosphine side as ligands **1e** and **1f** (entries 5, 6) produce lower conversions than less hindered **1a** or **1d** (entries 1, 4). On the other hand, increasing the ligand flexibility does not seem to exert a detrimental effect on either catalytic activity or regioselectivity as shown by comparing the performance of the Rh complex with ligand **3** (entry 8) to those obtained with ligand **1a**.

As expected, the enantioselectivity is very dependent on the phosphine–phosphite ligand used, from 19% ee obtained with ligand **5b** (entry 12) to a remarkable 71% ee afforded by **1f**

(17) See, for instance: (a) van Rooy, A.; Kamer, P. C. J.; van Leeuwen, P. W. N. M.; Goubitz, K.; Fraanje, J.; Veldman, N.; Spek, A. L. *Organometallics* **1996**, *15*, 835. (b) Van Rooy, A.; Orij, E. N.; Kamer, P. C. J.; van den Aardweg, F.; van Leeuwen, P. W. N. M. *J. Chem. Soc., Chem. Commun.* **1991**, 1096.

(16) Gridnev, I. D.; Higashi, N.; Asakura, K.; Imamoto, T. *J. Am. Chem. Soc.* **2000**, *122*, 7183.

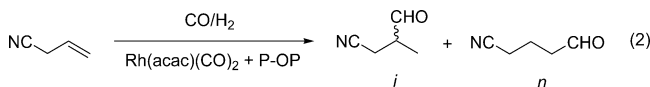
**Table 2. Allyl Cyanide Hydroformylation<sup>a</sup>**

entry	P-OP	% conversion	i:n	% ee (conf.)
1	<b>1a</b>	70	94:6	23 ( <i>S</i> )
2	<b>1c</b>	65	90:10	6 ( <i>R</i> )
3	<b>1d</b>	75	93:7	53 ( <i>S</i> )
4	<b>1e</b>	10	95:5	22 ( <i>S</i> )
5	<b>1f</b>	30	84:16	31 ( <i>S</i> )
6	<b>4a</b>	85	90:10	11 ( <i>S</i> )
7	<b>4b</b>	90	91:9	40 ( <i>R</i> )

<sup>a</sup> Reactions were carried out at 50 °C with an initial gas pressure of 20 bar, in toluene at a S/C = 1000 in a 750 mL reaction vessel. Conversion was determined by <sup>1</sup>H NMR and enantiomeric excess (ee) by chiral GC. Configuration was determined by comparison of optical rotation to the literature value.

(entry 6). However, the configuration of the aldehyde product seems to be driven by a rather complex correlation between the type of phosphine, phosphite, and backbone fragments. Indeed, despite all of the members of the **1** family having a phosphite group with *S* configuration, the ligands with a diarylphosphino group produce the aldehyde with *S* configuration (entries 1, 4–6), while the *R* enantiomer is predominant in the reactions performed with the dialkylphosphino ligands **1b** and **1c** (entries 2, 3). Interestingly, the aldehyde configuration changes, with respect to that obtained with **1a**, by using the ethylene bridged ligand **3**. On the other hand, reactions performed with the *P*-stereogenic ligands **4** and **5** indicate that the configuration of the phosphite group determines the chirality of the final product (entries 9–12). Like for ligand **1a**, for the pair of ligands **4** *S* phosphite favors the formation of the *S* product. Otherwise, for ligands **5** the preferred product for the *S* phosphite is *R*, as found for ligand **3**. No enantioselectivity enhancement was observed by using the *P*-stereogenic ligands **4** and **5** as compared to their nonstereogenic phosphine congeners **1** and **3**. This finding contrasts with the behavior of aminophosphine–phosphinite ligands for which an important increase in the enantioselectivity was observed by substituting the PPh<sub>2</sub> group with a stereogenic P(Ph)Me fragment.<sup>18</sup>

Phosphine–phosphites **1** and **4** have also been examined in the Rh-catalyzed hydroformylation of allyl cyanide (eq 2).<sup>19</sup> The results are reported in Table 2. Catalytic conversions up to 90% in 24 h were obtained (entry 7). In all cases, the regioselectivity was remarkably high, with a branched to linear ratio up to 15.7 with ligand **1a** (entry 1), while the enantioselectivity was from low to moderate, with the highest value (53% ee) for ligand **1d** (entry 3).



To obtain mechanistic information, we studied the hydroformylation reactions assisted by ligands **1a–1c**, **1e**, and **1f** by means of in situ HP-NMR spectroscopy, which allowed us to intercept hydride species of the formula RhH(P-OP)(CO)<sub>2</sub>. As previously reported,<sup>11a,b</sup> these complexes may be generated from the stoichiometric reaction of Rh(acac)(CO)<sub>2</sub> with the corresponding phosphine–phosphite upon heating the resulting mixture at 50–60 °C for 2–4 h under 20 bar of H<sub>2</sub>/CO (1:1). Selected <sup>31</sup>P{<sup>1</sup>H} and <sup>1</sup>H chemical shifts and coupling constants for these rhodium hydrides are collected in Table 3. With the exception of the derivative of **1e** (see below), all of the

(18) Ewalds, R.; Eggeling, E. B.; Hewat, A. C.; Kamer, P. C. J.; van Leeuwen, P. W. N. M.; Vogt, D. *Chem. Eur. J.* **2000**, *6*, 1496.

(19) (a) Lambers-Verstappen, M. M. H.; de Vries, J. G. *Adv. Synth. Catal.* **2003**, *345*, 478. (b) Cobley, C. J.; Gardner, K.; Klosin, J.; Praquin, C.; Hill, C.; Whiteker, G. T.; Zanolli-Gerosa, A. *J. Org. Chem.* **2004**, *69*, 4031.

complexes RhH(CO)<sub>2</sub>(**1**) exhibit in solution a single set of resonances, which is consistent either with the presence of a single complex in solution or with a fast interchange between several species. The <sup>31</sup>P{<sup>1</sup>H} NMR spectra of these complexes show the expected AMX (X = <sup>103</sup>Rh) spin system with resonances in the region of coordinated phosphines and phosphites with <sup>1</sup>J<sub>RhP</sub> of 95 and 235 Hz, respectively, and <sup>2</sup>J<sub>PP</sub> values of ca. 60 Hz, similar to those already reported for RhCl(CO)-(**1**) complexes.<sup>12a</sup>

At room temperature, the <sup>1</sup>H NMR spectrum of RhH(CO)<sub>2</sub>(**1b**) shows a doublet of doublets at –8.80 ppm with a <sup>1</sup>J<sub>HRh</sub> of 9.4 Hz and a <sup>2</sup>J<sub>HP</sub> of 117.5 Hz. The latter is due to the coupling of the hydride ligand to the phosphine phosphorus nucleus. Upon cooling, the chemical shifts and coupling constants did not change significantly. Interestingly, no coupling of the hydride to the phosphite P-atom was observed at any temperature, which is consistent with a *cis* disposition of the hydride and phosphite ligands in a trigonal bipyramidal coordination geometry where the phosphine group occupies an apical coordination site (structure **C**).<sup>11a</sup>

The rhodium–hydrido(dicarbonyl) complexes with ligands **1a** and **1f** showed a somewhat different behavior in the temperature range between 50 and –90 °C, which is consistent with scrambling of the two phosphorus atoms with respect to axial and equatorial positions of the bipyramidal structure. The value of the coupling constant <sup>1</sup>J<sub>HRh</sub> is around 10 Hz for both complexes in the temperature range investigated, pointing to an apical hydride with a *trans* phosphorus atom. Values of <sup>2</sup>J<sub>HP(phosphite)</sub> of 40 and 32 Hz were observed at 50 °C for the complexes stabilized by **1a** and **1f**, respectively. This coupling constant decreases with temperature and for RhH(CO)<sub>2</sub>(**1a**) has the value of 15.2 Hz at –60 °C. Extensive signal broadening precludes a reliable evaluation of <sup>2</sup>J<sub>HP(phosphite)</sub> below this temperature. Notably, the magnitude of <sup>2</sup>J<sub>HP(phosphine)</sub> increases from 90 Hz at 50 °C to 112 Hz at –90 °C. These observations are consistent with an equilibrium between species **C** and **D** for the rhodium hydride dicarbonyls derived from **1a** and **1f**.<sup>11b</sup> On the other hand, the spectroscopic data of RhH(CO)<sub>2</sub>(**1b**) provide a <sup>2</sup>J<sub>HP</sub> value of ca. 115 Hz for the *trans* hydride and phosphine groups, while previous studies of the BINAPHOS hydrido(dicarbonyl) report a <sup>2</sup>J<sub>HP</sub> value of 160 Hz.<sup>11a</sup> Finally, irrespective of the phosphine or phosphite, <sup>2</sup>J<sub>HP</sub> should be around 0–5 Hz for hydride and phosphorus groups occupying mutually *cis* positions of a trigonal bipyramid. Therefore, the observed <sup>2</sup>J<sub>HP</sub> values for the rhodium hydride dicarbonyls of **1a** and **1f** indicate a fast exchange between species **C** and **D** at 50 °C, with a prevalence of the former species, which is further on favored on decreasing the temperature. On the basis of the values of <sup>2</sup>J<sub>HP</sub>, a **C**:**D** ratio of ca. 4:1 at 50 °C can be estimated for both complexes.<sup>20</sup>

The isopropyl derivative RhH(CO)<sub>2</sub>(**1c**) exhibits a less clear behavior. The values of the <sup>2</sup>J<sub>HP</sub> coupling constants do not significantly change with temperature, as observed for Rh(H)-(CO)<sub>2</sub>(**1b**). Analogously, the <sup>2</sup>J<sub>HP(phosphine)</sub> maintains the characteristic values of a *trans* relation between the hydride and the phosphine ligands. However, <sup>2</sup>J<sub>HP(phosphite)</sub> is significantly higher than the near null value expected for a *cis* arrangement. These data may be ascribed to the presence of a mixture of species (**C** and **D**). Alternatively, the high value of the *cis* constant may be attributed to a distortion of species **C**<sup>11a</sup> from the ideal trigonal bipyramidal geometry due to steric congestion.

(20) Casey, C. P.; Paulsen, E. L.; Beuttenmueller, E. W.; Proft, B. R.; Petrovich, L. M.; Matter, B. A.; Powell, D. R. *J. Am. Chem. Soc.* **1997**, *119*, 11817.

Table 3. NMR Data for the Hydride Resonance of RhH(P–OP)(CO)<sub>2</sub> Complexes<sup>a</sup>

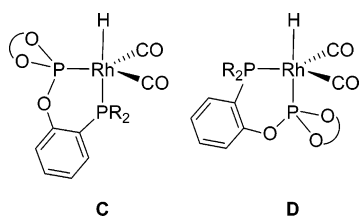
entry	P–OP	T (°C)	$\delta_{\text{HRh}}$	$^1J_{\text{HRh}}^b$	$\delta_{\text{PC}}$	$^2J_{\text{HPC}}$	$\delta_{\text{PO}}$	$^2J_{\text{HPO}}$
1	<b>1a</b>	50	-9.10	10.1	19.0	92.5	159.2	40
2		25	-9.01	9.7	20.7	96.3	161.6	33
3		-90	-8.64	br d	21.9	111.8	165.5	br d
4	<b>1b</b>	50	-8.88	br d	-19.2	117.7	158.3	
5		25	-8.80	9.4	-18.8	117.5	159.3	
6		-90	-8.32	10.0	-17.2	113.8	162.9	
7	<b>1c</b>	50	-8.96	10.1	35.6	91.1	151.4	50
8		25	-8.78	10.3	34.7	92.4	151.9	47
9		-90	-8.29	br d	33.6	97.4	151.9	br d
10	<b>1e</b>	50	-9.37	8.9	12.0	75.6	156.0	53
11 <sup>c</sup>		25	-9.33	8.8	18.5	br	161.4	br
					7.6	br	154.4	br
12 <sup>d</sup>		-90	-8.61	br	21.3	120	157.2	
			-9.33	br	3.6	108	152.8	
13	<b>1f</b>	50	-9.63	10.3	5.1	89.6	155.3	32
14		25	-9.53	8.4	5.1	101.5	156.2	28
15		-90	-9.6	br d	5.5	112.9	157.2	br d

<sup>a</sup> In toluene-*d*<sub>8</sub>. Chemical shifts in ppm, coupling constants in Hz. <sup>b</sup> br d: broad doublet in the <sup>1</sup>H NMR spectrum. <sup>c</sup> One group of signals in the <sup>1</sup>H NMR spectrum and two groups of resonances in the <sup>31</sup>P{<sup>1</sup>H} NMR spectrum. <sup>d</sup> Two groups of NMR signals in the <sup>1</sup>H and <sup>31</sup>P{<sup>1</sup>H} NMR spectra.

In this respect, it should be noted that, as the coupling constant  $^2J_{\text{HP(phosphite)}}$  changes from ca. 0 to 160 Hz in going from *cis*-hydride–phosphite to *trans*-hydride–phosphite, a small distortion of the geometry may produce a significant increase in the value of  $^2J_{\text{HP(phosphite)}}$ . Additional support to this hypothesis is provided by stereoelectronic considerations. Indeed, according to literature data, the more  $\sigma$ -donor group (phosphine) should occupy the apical position with the equatorial position occupied by the better  $\pi$ -acceptor (phosphite).<sup>21</sup> Following this assumption, the hydride complex with ligand **1b** should have an electronic preference for structure **C**, in good accord with the experimental observations. In contrast, for derivatives of the less basic ligands **1a** and **1f**, this preference is less pronounced and structure **D** becomes, as observed, energetically competitive. Finally, as ligand **1c** contains the most basic phosphine group of the series,<sup>12a</sup> it is reasonable to expect a marked preference for structure **C** for the related rhodium hydrido(dicarbonyl) complex.

At variance with the rest of the hydrides investigated, the *o*-tolyl derivative RhH(CO)<sub>2</sub>(**1e**) displays two groups of signals in the <sup>31</sup>P{<sup>1</sup>H} NMR spectrum at -90 °C, with  $^1J_{\text{RHP}}$  and  $^2J_{\text{PP}}$  values similar to those for RhH(CO)<sub>2</sub>(**1a**) at the same temperature. In addition, the <sup>1</sup>H NMR spectrum acquired at -90 °C shows two broad doublets with  $^2J_{\text{HP}}$  of ca. 120 and 108 Hz. These data can be interpreted with the existence of two type-**C** species. The occurrence of rotational isomers observed in PdCl<sub>2</sub>(**1e**) led us to propose that the two isomers observed for RhH(CO)<sub>2</sub>(**1e**) at low temperature differ in the orientation of the *o*-tolyl substituents.

The HP-NMR data therefore indicate a preference for structure **C** of (hydride)dicarbonyls derived from **1**. This coordination mode is also preferred by other phosphine–phosphites described by van Leeuwen<sup>11a</sup> and Claver,<sup>11b</sup> while the structure of type **D** is the preferred one by ligands of the BINAPHOS family.<sup>10b</sup>



The preferred apical coordination of the phosphine group deserves a further comment in view of the styrene hydroformy-

lation results. Previous studies on rhodium complexes with phosphine–phosphite ligands indicate that the concurrence of both coordinating functions is necessary to achieve a high enantiomeric excess, while the equatorial group mostly influences the enantioselectivity of the reaction.<sup>10,11</sup> Indeed, in the reactions catalyzed by the rhodium complexes with the ligands **4** and **5**, containing two stereogenic elements, the phosphite group determines the configuration of the branched aldehyde. On the other hand, this trend is not always preserved along the series investigated, as both the nature of the phosphine group and the backbone can affect the product configuration as well. Recently, detailed theoretical calculations on aminophosphine–phosphinite rhodium complexes (also displaying an apical–equatorial coordination mode) have identified the formation of  $\pi$ – $\pi$  stacking interactions between the apical aminophosphine and the bonded styrene as an important stereoregulating factor.<sup>22</sup> Therefore, it is not strictly correct to compare results obtained with ligands bearing dialkyl- and diarylphosphino groups. Concerning the latter, our present data show that a good enantioselectivity is observed in the hydroformylation of styrene with the catalyst containing the ligand **1f**, which possesses neither a *P*-stereogenic phosphine group nor a chiral backbone. Previous studies have demonstrated that ligands **1a**–**1f** are rather rigid due to interactions between the phenylene backbone and the bulky phosphite.<sup>12a</sup> As a consequence, ligands with PAR<sub>2</sub> groups display a propeller-like chiral arrangement of the aryl substituents typical of diphosphines with a chiral backbone, also observed in the structures of complexes **7**. On the other hand, earlier works on the ethane-based phosphine–phosphite ligand **3** demonstrated that this ligand displays a different aryl arrangement that switches the *face* and *edge* oriented phenyl rings around the plane defined by Rh and P atoms (Figure 5). From these considerations, it is possible that a similar  $\pi$ – $\pi$  stacking effect may operate in the present catalytic systems as well. Thus, the increased enantioselectivity in the hydroformylation of styrene found for the naphthyl catalyst in view of the higher interaction calculated between the substrate and model catalysts with PH<sub>2</sub>(1-naphthyl) with respect to PH<sub>2</sub>Ph analogues is not surprising.<sup>22</sup> Noteworthy, the naphthyl catalyst can benefit

(21) (a) Zuidema, E.; Daura-Oller, E.; Carbó, J. J.; Bo, C.; van Leeuwen, P. W. N. M. *Organometallics* **2007**, *26*, 2234. (b) Casey, C. P.; Paulsen, E. L.; Beuttenmueller, E. W.; Proft, B. R.; Matter, B. A.; Powell, D. R. *J. Am. Chem. Soc.* **1999**, *121*, 63.

(22) Carbó, J. J.; Lledós, A.; Vogt, D.; Bo, C. *Chem. Eur. J.* **2006**, *12*, 1457.

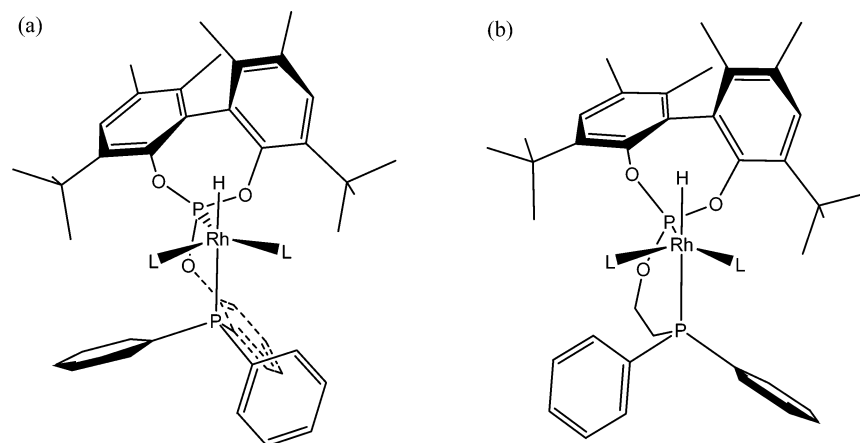


**Figure 5.** Structures of complexes  $\text{RhH}(\text{P}-\text{OP})\text{L}_2$  ( $\text{L} = \text{CO}$ , olefin).  $\text{P}-\text{OP} = \mathbf{1a}$  (a),  $\mathbf{3}$  (b).

**Table 4. Hydroformylation of Vinyl Naphthalenes**  
 $\text{Ar}-\text{CH}=\text{CH}_2$  with  $\text{P}-\text{OP}$ -Based Catalysts

entry	Ar	P-OP	% conversion (time)	i:n	% ee (conf.)
1	2-naphthyl	<b>1a</b>	100	98:2	44 (S)
2	2-naphthyl	<b>1f</b>	45	98:2	75 (S)
3	1-naphthyl	<b>1a</b>	100	95:5	68 (S)
4	1-naphthyl	<b>1f</b>	100	99:1	89 (S)

<sup>a</sup> Reactions were carried out at 50 °C for 24 h with an initial gas pressure of 20 bar, in toluene at a S/C = 1000 in a 750 mL reaction vessel. Conversion was determined by <sup>1</sup>H NMR and enantiomeric excess (ee) by chiral GC. Configuration was determined by comparison of optical rotation to the literature value.<sup>24</sup>

from a restricted rotation of the aryl substituents, which would facilitate a defined interaction between the aromatic rings.<sup>23</sup>

With the intention to confirm the positive role ascribed to the substrate to ligand aryl-aryl interaction for achieving higher enantioselectivities in the carbonylation of aryl-substituted alkenes, the hydroformylation of 1- and 2-vinyl naphthalenes has also been examined. The corresponding results are collected in Table 4. These data indicate that, while 2-vinyl naphthalene shows a small increase in the enantioselectivity as compared to styrene (entries 1, 2), 1-vinyl naphthalene gives significantly higher enantioselectivities than styrene (entries 3, 4). With catalyst **1a**, where the supposedly beneficial interaction between the 1-naphthyl and Ph substituents is still active, although with reversed reciprocal position of the aryl groups, a 68% ee was obtained (versus 43% ee in styrene hydroformylation with the same catalyst). Finally, the effect is maximized by confronting two  $\alpha$ -naphthyl substituents, and a significant increase up to 89% ee was observed.

### Conclusions

Rhodium(I) complexes bearing chiral phosphine-phosphite ligands have been evaluated in the hydroformylation of vinyl arenes and allyl cyanide. High regioselectivities, ranging from 93% to 98% in the branched aldehyde, were obtained with all substrates. The highest ee values observed in the hydroformylation of styrene and allyl cyanide were 71% and 53% ee, respectively. Structural studies on complexes **7a** and **7e** have shown the occurrence in solution of restricted rotation of the pseudoaxial tolyl group in the latter complex. HP-NMR studies have allowed us to determine the coordination mode of ligands of type **1** in the hydrido(dicarbonyl) species  $\text{RhH}(\text{CO})_2(\mathbf{1})$  formed in situ. This study has shown a clear preference for an axial-equatorial coordination of the bidentate ligand with the

phosphite group occupying an equatorial position. With regards to the influence of the structure of the diarylphosphino groups on product configuration, the  $\pi$ - $\pi$ /aryl-aryl interaction between phosphine and olefin substituents seems to exert an important role. Consistently, 1-naphthyl substituents provided a significant enhancement on the selectivity. The highest enantioselectivity was 89% ee in the carbonylation of 1-vinyl naphthalene with the rhodium catalyst bearing the naphthyl-substituted ligand **1f**.

### Experimental Section

**General Comments.** All reactions and manipulations were performed under nitrogen or argon, either in a Braun Labmaster 100 glovebox or using standard Schlenk-type techniques. All solvents were distilled under nitrogen using the following dessicants: sodium-benzophenone-ketyl for benzene, diethylether ( $\text{Et}_2\text{O}$ ), and tetrahydrofuran (THF); sodium for petroleum ether and toluene;  $\text{CaH}_2$  for dichloromethane ( $\text{CH}_2\text{Cl}_2$ ); and NaOMe for methanol (MeOH). Enantiomers of 3,3'-di-*tert*-butyl-5,5',6,6'-tetramethyl-2,2'-bisphenoxyphosphorus chloride and ligands **1a-1e**, **2-5** were prepared as described previously.<sup>12,13</sup> *o*-Anisyl-di-1-naphthylphosphine was prepared according to a literature procedure.<sup>14</sup> 1-Vinyl naphthalene was purified by extraction in *n*-hexane. All other reagents were purchased from commercial suppliers and used as received. NMR spectra were obtained on a Bruker DPX-300, DRX-400, or DRX-500 spectrometer. <sup>31</sup>P{<sup>1</sup>H} NMR shifts were referenced to external 85%  $\text{H}_3\text{PO}_4$ , while <sup>13</sup>C-{<sup>1</sup>H} and <sup>1</sup>H shifts were referenced to the residual signals of deuterated solvents. All data are reported in ppm downfield from  $\text{Me}_4\text{Si}$ . All NMR measurements were carried out at 25 °C, unless otherwise stated. HP-NMR experiments were carried out on a Bruker ACP 200 spectrometer, using a 10 mm tube (Saphikon sapphire tube; titanium high-pressure charging head constructed at the ICCOM).<sup>25</sup> GC analyses were performed by using a Hewlett-Packard model HP 6890 chromatograph. HPLC analyses were performed by using a Waters 2690 system. HRMS data were obtained using a Jeol JMS-SX 102A mass spectrometer. Elemental analysis was run by the Analytical Service of the Instituto de Investigaciones Químicas in a Leco CHNS-932 elemental analyzer. Optical rotations were measured on a Perkin-Elmer model 341 polarimeter. IR spectra were acquired on a Bruker Vector 22 instrument.

**Synthesis of 2-Hydroxyphenyldi(1-naphthyl)phosphine.** To a solution of *o*-anisyl-di-1-naphthylphosphine (1.22 g, 3.1 mmol) in  $\text{CH}_2\text{Cl}_2$  (50 mL) cooled at -78 °C was added  $\text{BBr}_3$  (0.70 mL, 7.6 mmol). The resulting solution was left to warm to room temperature

(23) Kojima, T.; Hayashi, K.; Matsuda, Y. *Inorg. Chem.* **2004**, *43*, 6793.

(24) Menicagli, R.; Piccolo, O.; Lardicci, L.; Wis, M. L. *Tetrahedron* **1979**, *35*, 1301.

(25) Bianchini, C.; Meli, A.; Traversi, A. Ital Patent FI A000025, 1997.

and stirred for 16 h. The solution was evaporated, and a portion of toluene (25 mL) was added and re-evaporated to ensure complete elimination of volatiles. The remaining solid was treated with MeOH (20 mL) at 0 °C and stirred for 2 days at room temperature. The mixture was evaporated to dryness, resulting in a white solid that was suspended in Et<sub>2</sub>O (30 mL). Next, NEt<sub>3</sub> (0.70 mL, 4.5 mmol) was added, and the suspension was stirred for 2 h, filtered, and the solvent was evaporated to dryness, resulting in the compound as a white foamy solid (0.54 g, 45%). IR (nujol mull, cm<sup>-1</sup>): 3492 (s, ν(OH)). <sup>1</sup>H NMR (CDCl<sub>3</sub>, 300 MHz): δ 6.29 (brs, 1H, OH), 6.74–6.91 (m, 2H), 6.97 (t, *J*<sub>HH</sub> = 6.0 Hz, 1H), 7.08 (t, *J*<sub>HH</sub> = 6.0 Hz, 2H), 7.25–7.38 (m, 3H), 7.39–7.55 (m, 4H), 7.80–7.92 (m, 4H), 8.34 (dd, *J*<sub>HH</sub> = 8.0, 4.0 Hz, 2H). <sup>31</sup>P{<sup>1</sup>H} NMR (CDCl<sub>3</sub>, 121 MHz): δ -47.0. <sup>13</sup>C{<sup>1</sup>H} NMR (CDCl<sub>3</sub>, 75 MHz): δ 115.9 (CH), 119.1 (C<sub>q</sub> arom), 121.6 (CH), 126.0 (2 CH), 126.2 (s, CH), 126.4 (s, 2 CH), 126.6 (s, CH), 126.8 (s, 2 CH), 129.0 (s, 2 CH), 130.3 (s, 2 CH), 131.2 (d, *J*<sub>CP</sub> = 5.0 Hz, 2 C<sub>q</sub>), 132.1 (CH), 133.0 (2 CH), 133.9 (d, *J*<sub>CP</sub> = 5.0 Hz, 2 C<sub>q</sub> arom), 135.4 (C<sub>q</sub>), 135.5 (C<sub>q</sub> arom), 135.8 (d, *J*<sub>CP</sub> = 4.0 Hz, CH), 159.6 (d, *J*<sub>CP</sub> = 19.0 Hz, C<sub>q</sub> arom). HRMS (CI): *m/z* 378.1172, [M]<sup>+</sup> (exact mass calculated for C<sub>26</sub>H<sub>19</sub>OP: 378.1174).

**Synthesis of the Phosphine–Phosphite Ligand 1f.** To a solution of (*S*)-3,3'-di-*tert*-butyl-5,5',6,6'-tetramethyl-2,2'-bisphenoxyphosphorus chloride (0.49 g, 1.27 mmol) and NEt<sub>3</sub> (0.3 mL, 1.9 mmol) in toluene (40 mL) was added a solution of 2-hydroxyphenyldi(1-naphthyl)phosphine (0.48 g, 1.27 mmol) in toluene (20 mL). The resulting suspension was stirred for 16 h, filtered, volatiles evaporated, and the remaining residue treated with Et<sub>2</sub>O (20 mL), filtered through a pad of neutral alumina, and the solution obtained was evaporated, yielding **1f** as a white foamy solid (0.44 g, 45%). [α]<sub>D</sub><sup>20</sup> = 262 (c 1.0, THF). <sup>1</sup>H NMR (CDCl<sub>3</sub>, 500 MHz): δ 1.14 (s, 9H, CMe<sub>3</sub>), 1.40 (s, 9H, CMe<sub>3</sub>), 1.82 (s, 3H, Me), 1.86 (s, 3H, Me), 2.23 (s, 3H, Me), 2.29 (s, 3H, Me), 6.72 (m, 1H, H arom), 6.90 (t, *J*<sub>HH</sub> = 7.0 Hz, H arom), 6.96 (m, 3H, H arom), 7.03 (s, 1H, H arom), 7.24 (m, 4H, H arom), 7.33 (t, *J*<sub>HH</sub> = 7.0 Hz, 1H, H arom), 7.39 (t, *J*<sub>HH</sub> = 7.0 Hz, 1H, H arom), 7.47 (q, *J*<sub>HH</sub> = 8.0 Hz, 2H, H arom), 7.83 (dd, *J*<sub>HH</sub> = 6.2 Hz, 2H, H arom), 7.87 (dd, *J*<sub>HH</sub> = 8.2 Hz, 2H, H arom), 8.40 (m, 2H, H arom). <sup>31</sup>P{<sup>1</sup>H} NMR (313 K, CDCl<sub>3</sub>, 202 MHz): δ -35.0 (d, *J*<sub>PP</sub> = 40.0 Hz, PC), 129.2 (brs, PO). <sup>13</sup>C{<sup>1</sup>H} NMR (CDCl<sub>3</sub>, 126 MHz): δ 16.7 (Ar–Me), 16.8 (Ar–Me), 20.5 (Ar–Me), 20.5 (Ar–Me), 31.1 (CMe<sub>3</sub>), 31.2 (d, *J*<sub>CP</sub> = 5.0 Hz, CMe<sub>3</sub>), 34.5 (CMe<sub>3</sub>), 34.7 (CMe<sub>3</sub>), 122.0 (brs, CH arom), 124.6 (CH arom), 125.7 (CH arom), 125.8 (CH arom), 125.8 (CH arom), 125.9 (CH arom), 126.1 (CH arom), 126.8 (d, *J*<sub>CP</sub> = 27.0 Hz, CH arom), 127.0 (d, *J*<sub>CP</sub> = 26.0 Hz, CH arom), 127.8 (CH arom), 128.2 (d, *J*<sub>CP</sub> = 11.0 Hz, C<sub>q</sub> arom), 128.3 (CH arom), 128.4 (CH arom), 128.5 (CH arom), 129.3 (2 CH arom), 130.3 (CH arom), 130.6 (C<sub>q</sub> arom), 131.6 (C<sub>q</sub> arom), 132.4 (d, *J*<sub>CP</sub> = 5.0 Hz, C<sub>q</sub> arom), 132.7 (CH arom), 132.9 (CH arom), 133.5 (CH arom), 133.7 (C<sub>q</sub> arom), 134.2 (C<sub>q</sub> arom), 135.2 (C<sub>q</sub> arom), 135.4 (C<sub>q</sub> arom), 135.6 (C<sub>q</sub> arom), 135.7 (C<sub>q</sub> arom), 137.6 (C<sub>q</sub> arom), 138.4 (C<sub>q</sub> arom), 144.7 (C<sub>q</sub> arom), 145.3 (d, *J*<sub>CP</sub> = 4.0 Hz, C<sub>q</sub> arom), 154.6 (d, *J*<sub>CP</sub> = 16.0 Hz, C<sub>q</sub> arom). HRMS (FAB): *m/z* 760.3250, [M]<sup>+</sup> (exact mass calculated for C<sub>50</sub>H<sub>50</sub>O<sub>3</sub>P<sub>2</sub>: 760.3235).

**Synthesis of the Complex PdCl<sub>2</sub>(1a) (7a).** To a solution of PdCl<sub>2</sub>(MeCN)<sub>2</sub> (0.052 g, 0.2 mmol) in toluene (5 mL) was added a solution of **1a** (0.139 g, 0.21 mmol) in toluene (5 mL). The mixture was stirred for 3 h, and then the solvent was removed under reduced pressure. The resulting solid was dissolved in CH<sub>2</sub>Cl<sub>2</sub> (10 mL) and filtered through Celite. The obtained solution was concentrated up to one-fourth of its original volume, and *n*-hexane (30 mL) was added to precipitate the product. The resulting solid was filtered off, washed with *n*-hexane (3 × 20 mL), and dried under vacuum. Yellow solid (0.10 g, 60%). <sup>1</sup>H NMR (CDCl<sub>3</sub>, 500 MHz): δ 1.05 (s, 9H, CMe<sub>3</sub>), 1.34 (s, 9H, CMe<sub>3</sub>), 1.79 (s, 3H, Me), 1.80 (s, 3H, Me), 2.21 (s, 3H, Me), 2.26 (s, 3H, Me), 6.67 (t, *J*<sub>HH</sub> = 7.0 Hz, 1H, H arom), 6.83 (m, 1H, H arom), 7.11 (s, 1H, H

arom), 7.13 (s, 1H, H arom), 7.19 (t, *J*<sub>HH</sub> = 8.0 Hz, 1H, H arom), 7.41 (m, 6H, H arom), 7.53 (m, 3H, H arom), 7.79 (dd, *J*<sub>HH</sub> = 13.0, 7.0 Hz, 2H, H arom). <sup>31</sup>P{<sup>1</sup>H} NMR (C<sub>6</sub>D<sub>6</sub>, 162 MHz): δ 11.5 (d, *J*<sub>PP</sub> = 16.0 Hz, PC), 113.2 (d, PO). <sup>13</sup>C{<sup>1</sup>H} NMR (CD<sub>2</sub>-Cl<sub>2</sub>, 126 MHz): δ 16.7 (Ar–Me), 17.0 (Ar–Me), 20.6 (2 Ar–Me), 31.2 (CMe<sub>3</sub>), 32.0 (CMe<sub>3</sub>), 34.7 (CMe<sub>3</sub>), 34.9 (CMe<sub>3</sub>), 118.3 (dd, *J*<sub>CP</sub> = 56, 12 Hz, C<sub>q</sub> arom), 122.7 (d, *J*<sub>CP</sub> = 3.0 Hz, CH arom), 125.1 (s, C<sub>q</sub> arom), 125.5 (C<sub>q</sub> arom), 126.2 (C<sub>q</sub> arom), 126.5 (d, *J*<sub>CP</sub> = 7.0 Hz, CH arom), 126.7 (C<sub>q</sub> arom), 127.9 (C<sub>q</sub> arom), 128.7 (CH arom), 128.8 (CH arom), 128.9 (CH arom), 129.0 (CH arom), 129.2 (CH arom), 129.3 (CH arom), 131.9 (d, *J*<sub>CP</sub> = 2.0 Hz, CH arom), 132.4 (d, *J*<sub>CP</sub> = 2.0 Hz, CH arom), 133.8 (C<sub>q</sub> arom), 134.1 (CH arom), 134.2 (CH arom), 134.3 (CH arom), 134.5 (CH arom), 134.6 (CH arom), 134.7 (CH arom), 134.7 (C<sub>q</sub> arom), 136.0 (C<sub>q</sub> arom), 136.7 (d, *J*<sub>CP</sub> = 4.0 Hz, C<sub>q</sub> arom), 137.5 (C<sub>q</sub> arom), 145.1 (d, *J*<sub>CP</sub> = 8.0 Hz, C<sub>q</sub> arom), 145.4 (d, *J*<sub>CP</sub> = 15.0 Hz, C<sub>q</sub> arom), 153.2 (d, *J*<sub>CP</sub> = 8.0 Hz, C<sub>q</sub> arom). Anal. Calcd for C<sub>42</sub>H<sub>46</sub>Cl<sub>2</sub>O<sub>3</sub>P<sub>2</sub>-Pd: C, 60.2; H, 5.5. Found: C, 60.1; H, 5.6.

**Synthesis of the Complex PdCl<sub>2</sub>(1e) (7e).** This compound was prepared following a synthetic procedure analogous to that described for **7a**, obtaining a yellow solid with 65% yield. Compound **7e** exists in solution as a mixture of rotational isomers (A and B) in a 0.7:1 ratio.<sup>26</sup> <sup>1</sup>H NMR (C<sub>6</sub>D<sub>6</sub>, 400 MHz): δ 1.13 (s, 9H, CMe<sub>3</sub> B), 1.19 (s, 9H, CMe<sub>3</sub> A), 1.48 (s, 12H, CMe<sub>3</sub> A and C<sub>6</sub>H<sub>4</sub>Me A), 1.50 (s, 9H, CMe<sub>3</sub> B), 1.67 (s, 3H, Me–ArO B), 1.67 (s, 3H, Me–ArO A), 1.72 (s, 3H, Me–ArO A), 1.76 (s, 3H, Me–ArO B), 1.97 (s, 3H, Me–ArO B), 1.99 (s, 3H, Me–ArO A), 2.09 (s, 3H, Me–ArO B), 2.09 (s, 3H, Me–ArO A), 2.81 (s, 3H, C<sub>6</sub>H<sub>4</sub>Me A), 2.86 (s, 3H, C<sub>6</sub>H<sub>4</sub>Me B), 3.35 (s, 3H, C<sub>6</sub>H<sub>4</sub>Me B), 6.53 (m, 6H, 3 H arom A and 3 H arom B), 6.73 (m, 6H, 3 H arom A and 3 H arom B), 6.96 (m, 7H, 3 H arom A and 4 H arom B), 7.11 (m, 4H, 2 H arom A and 2 H arom B), 7.21 (s, 1H, H arom B), 7.23 (s, 1H, H arom A), 7.27 (1H, H arom B), 7.28 (s, 1H, H arom A), 9.57 (brs, 1H, H arom A). <sup>31</sup>P{<sup>1</sup>H} NMR (CDCl<sub>3</sub>, 162.1 MHz): δ 1.3 (d, P–C B), 10.2 (brs, PC A), 109.1 (d, *J*<sub>PP</sub> = 15.0 Hz, PO B), 112.2 (brs, PO A). <sup>13</sup>C{<sup>1</sup>H} NMR (CDCl<sub>3</sub>, 75.5 MHz): δ 16.6 (s, Ar–Me, B), 16.6 (s, Ar–Me, A), 16.8 (s, Ar–Me, B), 16.9 (s, Ar–Me, A), 20.4 (s, 2 Ar–Me, B), 20.4 (s, 2 Ar–Me, A), 20.5 (s, 2 Me, B), 20.5 (s, 2 Me, A), 22.7 (d, *J*<sub>CP</sub> = 3.0 Hz, Ar–Me, A), 24.3 (d, *J*<sub>CP</sub> = 9.0 Hz, Ar–Me, A), 24.4 (d, *J*<sub>CP</sub> = 9.0 Hz, Ar–Me, B), 26.4 (d, *J*<sub>CP</sub> = 9.0 Hz, Ar–Me, B), 30.7 (s, CMe<sub>3</sub>, A), 30.9 (s, CMe<sub>3</sub>, B), 31.8 (s, CMe<sub>3</sub>, B), 31.8 (s, CMe<sub>3</sub>, A), 34.4 (s, CMe<sub>3</sub>, B), 34.4 (s, CMe<sub>3</sub>, A), 34.7 (s, CMe<sub>3</sub>, B), 34.7 (s, CMe<sub>3</sub>, A), 118.9 (dd, *J*<sub>CP</sub> = 58, 11 Hz, C<sub>q</sub> arom), 122.4 (s, C<sub>q</sub> arom), 123.2 (m, CH arom), 123.4 (m, CH arom), 125.0 (dd, *J*<sub>CP</sub> = 55, 4 Hz, C<sub>q</sub> arom), 126.1 (s, CH arom), 126.3 (s, CH arom), 126.4 (s, CH arom), 126.5 (s, CH arom), 127.4 (m, CH arom), 127.7 (s, C<sub>q</sub> arom), 128.5 (s, CH arom), 128.8 (s, 2 CH arom), 129.2 (m, C<sub>q</sub> arom), 131.7 (s, CH arom), 131.8 (s, CH arom), 131.9 (s, CH arom), 132.1 (s, CH arom), 132.2 (s, CH arom), 132.5 (s, CH arom), 132.6 (s, CH arom), 132.9 (s, CH arom), 133.0 (s, CH arom), 133.3 (s, CH arom), 133.4 (s, CH arom), 133.6 (s, C<sub>q</sub> arom), 133.7 (s, C<sub>q</sub> arom), 133.8 (s, C<sub>q</sub> arom), 134.2 (s, CH arom), 135.7 (s, C<sub>q</sub> arom), 135.7 (s, C<sub>q</sub> arom), 135.9 (s, C<sub>q</sub> arom), 136.4 (m, C<sub>q</sub> arom), 137.1 (m, C<sub>q</sub> arom), 141.2 (m, C<sub>q</sub> arom), 142.1 (s, C<sub>q</sub> arom), 143.0 (d, *J*<sub>CP</sub> = 11.0 Hz, C<sub>q</sub> arom), 143.7 (d, *J*<sub>CP</sub> = 11.0 Hz, C<sub>q</sub> arom), 145.2–145.9 (m, C<sub>q</sub> arom), 152.6 (dd, *J*<sub>CP</sub> = 8.3 Hz, C<sub>q</sub> arom), 153.2 (d, *J*<sub>CP</sub> = 8.0 Hz, C<sub>q</sub> arom). Anal. Calcd for C<sub>44</sub>H<sub>52</sub>Cl<sub>2</sub>O<sub>3</sub>P<sub>2</sub>Pd·CH<sub>2</sub>Cl<sub>2</sub>: C, 56.8; H, 5.5. Found: C, 56.4; H, 5.4.

**Procedure for Catalytic Hydroformylation Reactions. (a) Styrene and Allyl Cyanide.** A 750 mL Parr reaction vessel that holds six kilmax 35 mL tubes in a Teflon rack was introduced in a glovebox. Each tube was charged with styrene (0.78 g, 7.5 mmol) or allyl cyanide (0.50 g, 7.5 mmol) and Rh(acac)(CO)<sub>2</sub> (2 mg, 0.008

(26) Because of the complexity of the <sup>1</sup>H NMR spectra, only NMR signals of aliphatic groups have been assigned. In the <sup>1</sup>H NMR spectra, the intensities are calibrated to normalized unit value per each isomer.



Table 5. Summary of Crystallographic Data and Structure Refinement Results for 7a and 7e

	7a	7e
chem formula	C <sub>203</sub> H <sub>224</sub> Cl <sub>8</sub> O <sub>12</sub> P <sub>8</sub> Pd <sub>4</sub> [4(C <sub>42</sub> H <sub>46</sub> Cl <sub>2</sub> O <sub>3</sub> P <sub>2</sub> Pd), 5(C <sub>7</sub> H <sub>8</sub> )]	C <sub>123</sub> H <sub>140</sub> Cl <sub>4</sub> O <sub>6</sub> P <sub>4</sub> Pd <sub>2</sub> [2(C <sub>44</sub> H <sub>50</sub> Cl <sub>2</sub> O <sub>3</sub> P <sub>2</sub> Pd), 5(C <sub>7</sub> H <sub>8</sub> )]
fw	3812.78	2192.83
cryst size, mm	0.26 × 0.18 × 0.09	0.22 × 0.20 × 0.12
crystal system	monoclinic	triclinic
space group	P2 <sub>1</sub>	P1
a, Å	21.3901(11)	10.4905(6)
b, Å	10.2591(4)	14.6466(9)
c, Å	23.6159(12)	18.4648(11)
α, deg	90	101.028(2)
β, deg	111.5820(10)	96.166(2)
γ, deg	90	92.380(2)
V, Å <sup>3</sup>	4819.0(4)	2763.0(3)
Z	1	1
D <sub>calcd</sub> , g cm <sup>-3</sup>	1.314	1.318
μ, mm <sup>-1</sup>	0.602	0.535
F(000)	1978	1146
θ range	2.56–26.18°	2.90–30.58°
no. of measd reflns	26 937	74 197
no. of unique reflns	22 869 (R <sub>int</sub> = 0.0317)	31 966 (R <sub>int</sub> = 0.0454)
min, max transm fact	0.8592, 0.9478	0.8915, 0.9386
no of data/restraints/param	22 869/347/1093	31 966/1299/1452
R <sub>1</sub> (F) [F <sup>2</sup> > 2σ(F <sup>2</sup> )] <sup>a</sup>	0.0646	0.0447
observed reflections	15 866	26 744
wR <sub>2</sub> (F <sup>2</sup> ) <sup>b</sup> (all data)	0.1823	0.1115
S <sup>c</sup> [all data]	1.037	0.990
absolute structure parameter <sup>d</sup>	−0.03(3)	

<sup>a</sup>  $R_1(F) = \sum(|F_o| - |F_c|) / \sum|F_o|$  for the observed reflections [ $F^2 > 2\sigma(F^2)$ ]. <sup>b</sup>  $wR_2(F^2) = \{\sum[w(F_o^2 - F_c^2)^2] / \sum w(F_o^2)^2\}^{1/2}$ . <sup>c</sup>  $S = \{\sum[w(F_o^2 - F_c^2)^2] / (n - p)\}^{1/2}$ ;  $n$  = number of reflections,  $p$  = number of parameters. <sup>d</sup> Flack, H. D. *Acta Crystallogr.* **1983**, A39, 876–881.

mmol) and 4 equiv of the corresponding phosphine–phosphite dissolved in toluene (7 mL) and a magnetic stirrer. The reactor was then removed from the glovebox, purged three times with a 1:1 mixture of H<sub>2</sub>/CO, followed by pressurizing it to 20 bar and heated to 50 °C. The reaction solutions were stirred for the desired reaction time. Next, the reactor was slowly depressurized, and conversion and iso/*n* ratio were determined by <sup>1</sup>H NMR from an aliquot of the resulting solution. The mixture of aldehydes was then obtained by the evaporation of the solvent to dryness. Styrene hydroformylation: 2-Phenylpropanal was oxidized to the corresponding carboxylic acid<sup>10a</sup> and analyzed by GC (Chrompack β-236M, 170 °C (5 min), then 10 °C/min up to 180 °C (5 min), 28.0 psi He) (*S*)  $t_1$  = 3.60 min, (*R*)  $t_2$  = 3.68 min. Allyl cyanide hydroformylation: The enantiomeric excess was analyzed by GC (Astec Chiraldex A-TA 30 m, 90 °C (7 min), 5 °C/min up to 150 °C (5 min), 24.5 psi He) (*S*)  $t_1$  = 13.20 min, (*R*)  $t_2$  = 13.60 min. **(b) Vinyl Naphthalenes.** These olefins were hydroformylated following the procedure described above using olefin (598 mg, 3.9 mmol), Rh(acac)(CO)<sub>2</sub> (1 mg, 0.004 mmol), and 4 equiv of the corresponding phosphine–phosphite dissolved in toluene (4 mL). 1-Vinyl naphthalene hydroformylation: The product aldehyde was reduced to the corresponding alcohol<sup>27</sup> and analyzed as follows by HPLC (Chiralcel OK, 30 °C, *n*-hexane/2-propanol (99:1), flow 1.0 mL/min;  $t_R$  = 49.0 min (*R*),  $t_R$  = 53.5 min (*S*)). 2-Vinyl naphthalene hydroformylation: The obtained aldehyde was reduced to the corresponding alcohol as above and analyzed as follows by HPLC (Chiralcel OK, 30 °C, *n*-hexane/2-propanol (98:2), flow 1.0 mL/min;  $t_R$  = 33.7 min (*R*),  $t_R$  = 37.4 min (*S*)).

**HP-NMR Measurements. Preparation of NMR Samples of RhH(P–OP)(CO)<sub>2</sub>.** A 10 mm sapphire HP NMR tube was charged with a solution of Rh(acac)(CO)<sub>2</sub> (5.8 mg, 0.022 mmol) and P–OP (0.023 mmol) in toluene-*d*<sub>8</sub> (2.5 mL) under argon. After <sup>31</sup>P{<sup>1</sup>H} and <sup>1</sup>H NMR spectra were recorded to monitor the completeness

of the conversion into Rh(acac)(P–OP) complexes, the tube was purged three times with a 1:1 mixture of CO/H<sub>2</sub> and then pressurized to 20 bar with the same gas mixture. The tube was inserted in the probe and heated to 50 °C for 2–4 h, until Rh(acac)(P–OP) converted completely into the corresponding RhH(P–OP)(CO)<sub>2</sub> complexes. Both <sup>31</sup>P{<sup>1</sup>H} and <sup>1</sup>H NMR spectra of these latter complexes were carried out in the temperature range from 50 to −90 °C. Selected NMR data for RhH(P–OP)(CO)<sub>2</sub> complexes at 50, 25, and −90 °C are reported in Table 3.

**X-ray Structure Determinations.** Suitable crystals for a single-crystal X-ray structure analysis were grown by slow diffusion of *n*-hexane into a CH<sub>2</sub>Cl<sub>2</sub> solution of **7a** and **7e**. A single crystal, of each compound, of suitable size was mounted on a glass fiber using perfluoropolyether oil (FOMBLIN 140/13, Aldrich) in the cold N<sub>2</sub> stream. A summary of crystallographic data is reported in Table 5. Intensity data for complexes **7a** and **7e** were collected on a Bruker-AXS X8Kappa diffractometer equipped with an Apex-II CCD area detector, using a graphite monochromator Mo K<sub>α1</sub> ( $\lambda$  = 0.71073 Å) and a Bruker Cryo-Flex low-temperature device. A semiempirical absorption correction was applied (SADABS).<sup>28</sup> The structures were solved by direct methods (SIR-2002)<sup>29</sup> and refined against all  $F^2$  data by full-matrix least-squares techniques (SHELXTL-6.14).<sup>30,31</sup>

**Acknowledgment.** We gratefully acknowledge the Ministerio de Educación y Ciencia (CTQ2006-05527) and Fundación Ramón Areces for financial support. M.R. thanks the Ministerio de Educación y Ciencia for a FPU fellowship. Thanks are also due to EC through COST D17 Chemistry Action (WGD17/0003/00) to support the visit of A.S. at ICCOM CNR via the STSM Program.

**Supporting Information Available:** CIF files giving crystallographic data. This material is available free of charge via the Internet at <http://pubs.acs.org>.

OM700744B

(27) Halimjani, A. Z.; Saidi, M. R. *Synth. Commun.* **2005**, 35, 2271.

(28) Sheldrick, G. *SADABS*; Bruker AXS, Inc.: Madison, WI, 1999.

(29) Burla, M. C.; Camalli, M.; Carrozzini, B.; Cascarano, G. L.; Giacovazzo, C.; Polidori, G.; Spagna, R. *J. Appl. Crystallogr.* **2003**, 36, 1103.

(30) *SHELXTL 6.14*; Bruker AXS, Inc.: Madison, WI, 2000–2003.

(31) Sheldrick, G. M. *SHELX-97. Programs for crystal structure Analysis (release 97-2)*; Institut für Anorganische Chemie der universität: Göttingen, Germany, 1998.